

# The magnetospheric activity of bare strange quark stars

J. W. Yu and R. X. Xu

*School of Physics and State Key Laboratory of Nuclear Physics and Technology, Peking University, Beijing 100871, China*  
*email: J.W.Yu@pku.edu.cn, r.x.xu@pku.edu.cn*

Accepted 2011 January 23. Received 2011 January 16; in original form 2010 December 05

## ABSTRACT

In Ruderman & Sutherland (RS75) model, the normal neutron stars as pulsars bear a severe problem, namely the binding energy problem that both ions (e.g.,  $^{56}\text{Fe}$ ) and electrons on normal neutron star surface can be pulled out freely by the unipolar generator induced electric field so that sparking on polar cap can hardly occur. This problem could be solved within the Partially Screened Gap (PSG) model in the regime of neutron stars. However, in this paper we extensively study this problem in a bare strange quark star (BSS) model. We find that the huge potential barrier built by the electric field in the vacuum gap above polar cap could usually prevent electrons from streaming into the magnetosphere unless the electric potential of a pulsar is sufficiently lower than that at infinite interstellar medium. Other processes, such as the diffusion and thermionic emission of electrons have also been included here. Our conclusions are as follows: both positive and negative particles on a BSS's surface would be bound strongly enough to form a vacuum gap above its polar cap as long as the BSS is not charged (or not highly negative charged), and multi-accelerators could occur in a BSS's magnetosphere. Our results would be helpful to distinguish normal neutron stars and bare quark stars through pulsar's magnetospheric activities.

**Key words:** magnetospheric activities—pulsars: general

## 1 INTRODUCTION

Although pulsar-like stars have many different manifestations, they are populated mainly by rotation-powered radio pulsars. A lot of information about pulsar radiative process is inferred from the integrated and individual pulses, the sub-pulses, and even the micro-structures of radio pulses. Among the magnetospheric emission models, the user-friendly nature of Ruderman & Sutherland (1975; hereafter RS75) model is a virtue not shared by others (Shukre 1992).

In RS75 and its modified versions (e.g., Qiao & Lin 1998), a vacuum gap exists above polar cap of a pulsar, in which charged particles (electrons and positrons) are accelerated because of  $\mathbf{E} \cdot \mathbf{B} \neq 0$ . These accelerated charged particles, moving along the curved magnetic field lines, radiate curvature or inverse-Compton-scattering-induced high energy photons which are converted to  $e^\pm$  while propagating in strong magnetic field. A follow-up breakdown of the vacuum gap produces secondary electron-positron pairs plasma that radiate coherent radio emission. These models with gap-sparking provide a good framework to analyze observational phenomena, especially the drifting (Drake & Craft 1968; Deshpande & Rankin 1999; Vivekanand & Joshi 1999) and bi-drifting (Qiao et al. 2004) sub-pulses.

However, the RS75-like vacuum gap models work only in strict conditions: strong magnetic field and low temperature on surface of pulsars (e.g., Gil et al. 2008; Medin & Lai 2007). The necessary binding energy of positive ions (e.g.,  $^{56}\text{Fe}$ ) for RS75 model to work should be higher than  $\sim 10$  keV, while calculations showed that the cohesive energy of  $^{56}\text{Fe}$  at the neutron star surface is  $< 1$  keV (Fowlers et al. 1977; Lai 2001). This binding energy problem could be solved within a partially screened inner gap model (Gil et al. 2003, 2006a; Melikidze & Gil 2009) for normal neutron stars. Alternatively, it is noted that the binding energy could be sufficiently high if pulsars are bare strange quark stars (Xu & Qiao 1998; Xu et al. 1999, 2001) although strange stars were previously supposed to exist with crusts (Alcock et al. 1986). Certainly, it is very meaningful in the elementary strong interaction between quarks and the phases of cold quark matter that the binding energy problem could be solved by bare quark stars as pulsars (Xu 2009, 2010).

Though the ideas of solving the binding energy problem in BSS model were presented and discussed in some literatures, there is no comprehensive study with quantitative calculations up to now. In this paper, we are going to investigate the BSS model in quantitative details and show the physical picture of binding of particles on BSS's

surface. Our research results are that multi-accelerators could occur above the polar cap for (and only for) the curvature-radiation-induced (CR-induced) sparking normal pulsars (NPs), but for other cases, such as resonant inverse-Compton-scattering-induced (ICS-induced) sparking NPs and both CR-induced and ICS-induced millisecond pulsars (MSPs), particles on surface of BSSs are bound strongly enough to form vacuum gap and RS75-like models work well if pulsars are BSSs.

## 2 THE ACCELERATORS ABOVE POLAR CAPS OF BARE STRANGE QUARK STARS

On a BSS's surface, there are positively (*u*-quarks) and negatively (*d*- and *s*-quarks and electrons) charged particles. Quarks are confined by strong color interaction, whose binding energy could be considered as infinity when compared with the electromagnetic interaction, while electrons are bound by electromagnetic interaction. Therefore, in this paper we focus on the binding of electrons.

Let's discuss briefly the binding of electrons in the BSS model at first. On one hand, assuming the electric potential at the top of RS75 vacuum gap is the same as that of the interstellar medium, one could then have a potential barrier for electrons by integrating the gap electric field from top to bottom in the vacuum gap. This potential barrier could then prevent electrons streaming into magnetosphere. On the other hand, electrons above the stellar surface of BSS are described in the Thomas-Fermi model, in which the total energy of electrons on Fermi surface would be a constant,  $\phi_0$ . In previous work (e.g. Alcock et al. 1986), this constant is chosen to be zero,  $\phi_0 = 0$ , because they didn't consider the effect of spinning BSS with strong magnetic fields. Due to the unipolar generator effect, potential drop between different magnetic field lines is set up from pole to equatorial plane. This potential drop could result in different  $\phi_0$ , at different polar angle,  $\theta$ , and the total energy of electrons would then be obtained by choosing certain zero potential magnetic field line (i.e., at  $\theta_B$  or  $\theta_C$  in Fig. 1). Finally, comparing the total energy of electrons with the height of the potential barrier in vacuum gap, we can see whether electrons can stream into magnetosphere freely or not.

### 2.1 The energy of electrons on Fermi surface

The distribution of electrons in BSSs is described in the Thomas-Fermi model (Alcock et al. 1986). In this model, equilibrium of electrons in an external electric field assures that the total energy of each electron on Fermi surface is a constant,  $\phi_0$ . For the case of extremely relativistic degenerate electron gas, it gives (Alcock et al. 1986)

$$\epsilon(\vec{r}) = cp_F(\vec{r}) - e\varphi(\vec{r}) = \phi_0, \quad (1)$$

where  $\epsilon(\vec{r})$  is the total energy,  $cp_F(\vec{r})$  is the Fermi energy,  $-e\varphi(\vec{r})$  is the electrostatic potential energy of electrons and  $\phi_0$  is a constant, describing the potential energy of electrons in the Thomas-Fermi model at infinity.

On the other hand, the potential distribution of electrons on the star's surface due to the electric field induced by the rotating, uniformly magnetized star, for the sake of

simplicity, could be assumed and estimated as (Xu et al. 2006, Eq. 2 there)

$$V_i(\theta) \simeq 3 \times 10^{16} B_{12} R_6^2 P^{-1} \sin^2 \theta \text{ (V)} + V_0, \quad (2)$$

where  $B_{12} = B/(10^{12} \text{ G})$ , and  $R_6 = R/(10^6 \text{ cm})$  is the radius of a pulsar,  $P = 2\pi/\Omega$  is the pulsar period,  $\theta$  is the polar angle and  $V_0$  is another constant. In view of the distribution of electron above the surface of BSS extends only thousands of femtometers, the macroscopic potential drop between different magnetic field lines could be thought to be at infinity in the Thomas-Fermi model. And the potential energy related to Eq. 2,  $eV_i$ , could be regarded as the constant,  $\phi_0$ , in Eq. 1. By choosing the certain zero potential magnetic field line, we could obtain the total energy of electrons, namely  $eV_i$ . Two scenarios could be possible here. The first scenario is that we choose the critical field lines whose feet are at the same electric potential as the interstellar medium (Goldreich & Julian 1969) as the zero potential. We may also suggest a second choice that the zero potential should be at those magnetic field lines which separate annular and core regions determined by  $S_{AG} = S_{CG}$ , where  $S_{AG}$  and  $S_{CG}$ , are the stellar surface areas of annular region and core region, respectively. The second scenario is based on the idea that if particles with opposite charge stream into the magnetosphere with  $\rho_{G,J}$  in both regions, areas of this two regions should approximately be equal in order to keep the star not charging. The feet of the critical field lines and the magnetic field lines determined by  $S_{AG} = S_{CG}$  are designated as C and B, respectively (Fig. 1). For the above two scenarios, the total energy,  $\phi_i = eV_i$ , of electrons on the Fermi surface are given by

$$\phi_{i,C}(\theta) \simeq -3 \times 10^{10} B_{12} R_6^2 P^{-1} (\sin^2 \theta - \sin^2 \theta_C) \text{ MeV}, \quad (3)$$

and

$$\phi_{i,B}(\theta) \simeq -3 \times 10^{10} B_{12} R_6^2 P^{-1} (\sin^2 \theta - \sin^2 \theta_B) \text{ MeV}, \quad (4)$$

respectively, where  $\theta_C$  and  $\theta_B$  are polar angles of C and B (see Fig. 1). Equations 3 and 4 imply that the total energy of electrons is higher at the poles and decreases toward the equator for an 'antipulsar' ( $\vec{\Omega} \cdot \vec{B} > 0$ ), which means that electrons in different regions above a polar cap may behave differently.

### 2.2 The potential barrier of electrons in vacuum gap

In the following, we will consider the potential barrier of electrons in vacuum gap. Unlike RS75, we do calculations in situation of an 'antipulsar' whose magnetic axis is parallel to its spin axis. A schematic representation for 'antipulsar' is shown in Fig. 1. Assuming the electric potential at the top of RS75 vacuum gap is the same as that of the interstellar medium, we could get a potential barrier for electrons by integrating the gap electric field from top to bottom in the vacuum gap. This potential barrier, in one-dimensional approximation, is (RS75)

$$\phi_p(Z) = 2\pi \times 10^4 P^{-1} B_{12} (h_3 - Z_3)^2 \text{ MeV}, \quad (5)$$

where  $h_3 = h/(10^3 \text{ cm})$  is the height of vacuum gap,  $Z_3 = Z/(10^3 \text{ cm})$  is the space coordinate measuring height above the quark surface. This potential barrier may prevent

electrons injecting into pulsar's magnetosphere. The height of this potential barrier mainly depends on the height of vacuum gap which is determined by cascade mechanics of sparking, i.e., the CR-induced cascade sparking and the ICS-induced cascade sparking. In CR-induced cascade sparking model, the gap height is (RS75)

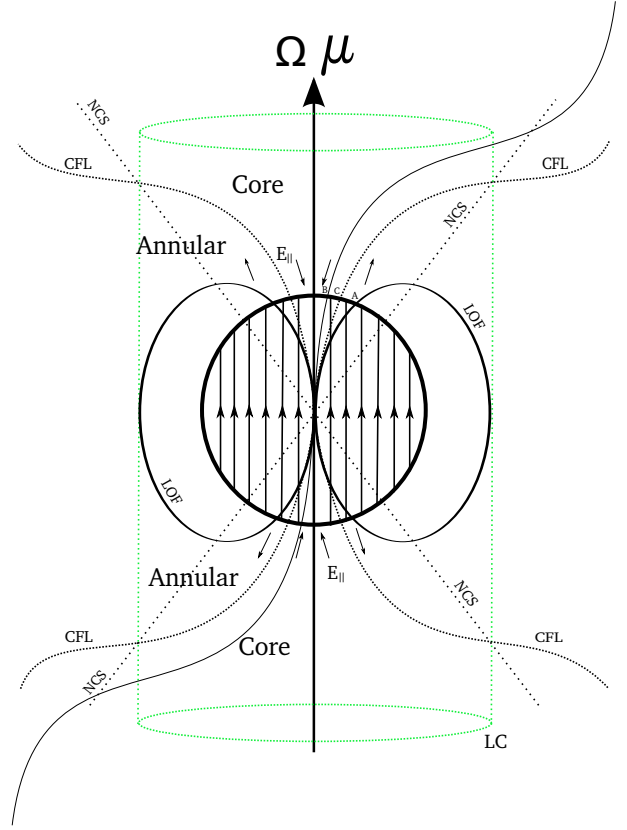
$$h_{\text{CR}} = 5 \times 10^3 \rho_6^{2/7} B_{12}^{-4/7} P^{3/7} \text{ cm}, \quad (6)$$

and in ICS-induced cascade sparking model, it is (Zhang et al. 2000)

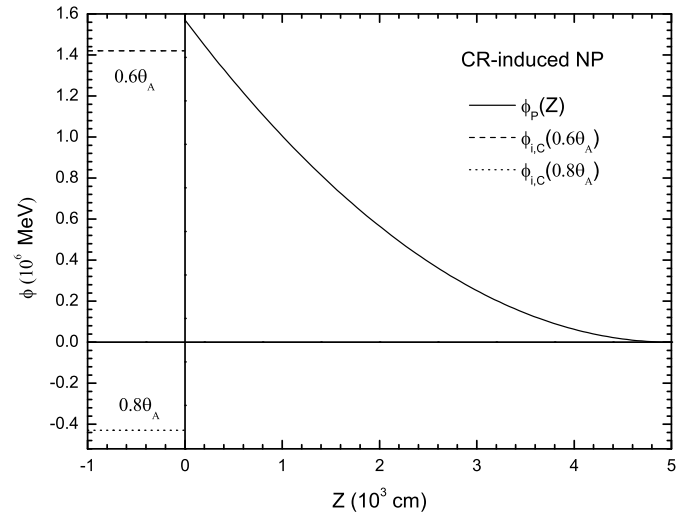
$$h_{\text{ICS}} = 2.79 \times 10^4 \rho_6^{4/7} B_{12}^{-11/7} P^{1/7} \text{ cm}. \quad (7)$$

In previous work of Gil et al. (2006), the heights of the vacuum gap of both CR-induced and ICS-induced sparking mechanism (Gil et al. 2006, Eqs. 21 and 22 there) are different from what we used in this work. In the PSG model, there was a partial flow of iron ions from the positively charged polar cap which coexist with the production of outflowing electron-positron plasmas. Such a charge-depleted acceleration region is also highly sensitive to both the critical ion temperature and the actual surface temperature of the polar cap (Gil et al. 2003). Differently, in our model, there is no flow of positively charged particles, namely quarks and also it is insensitive to the actual surface temperature. This means that there is no partial screened effect above polar cap of bare strange quark stars, namely the pure vacuum gap exists on polar cap of bare strange quark stars. That's the reason why we use Eqs. 6 and 7 in our calculation. Whether this choice of height of vacuum gap could result in different driftrate of subpulses or not is a complicated problem. We will discuss this problem very briefly in §3. The potential barrier of electrons in the gap for CR-induced cascade sparking model of typical normal pulsars (NPs) is plotted in Fig. 2, in which the total energy of electrons at the stellar surface, namely  $\phi_i$ , is illustrated at different polar angles. The situation of CR-induced cascade sparking of typical millisecond pulsars (MSPs) is similar to that of NPs but with greater height of potential barrier.

Comparing the potential barrier with total energy of electrons, we will explain behavior of electrons above polar cap. Namely, only electrons with energy greater than the potential barrier can escape into pulsar's magnetosphere. It is known that energy of electrons is a function of polar angle (Eqs. 3 and 4). As a result, there may be a critical polar angle,  $\theta_0$ , at which the energy of electrons equals the height of this potential barrier. Comparison between the total energy of electrons and the height of potential barrier on stellar surface for typical NPs of CR-induced sparking is shown in Fig. 3 ( $\theta_0$  does not exist for both ICS-induced sparking of NPs and MSPs, see Table. 1). The results are as follows: free flow status stays in the region of  $[0, \theta_0]$  and vacuum gap in  $[\theta_0, \theta_A]$  for 'antipulsars', where  $\theta_A$  is polar angle of the feet of the last open field lines (Fig. 1). We give the results of  $\theta_0$  in Table. 1 for both pulsar and 'antipulsar', and find that for the special case of CR-induced sparking NPs, free flow and vacuum gap could coexist above polar cap which differs from the previous scenario. The general case is that only vacuum gap exists.



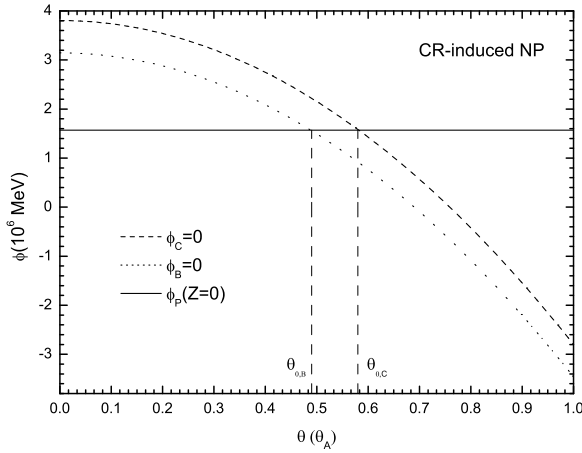
**Figure 1.** A schematic representation of the geometry of 'antipulsars'. CFL stands for the critical field lines, NCS for null charge surface, and LC for light cylinder. The enlarged arrows with opposite directions in annular region and core region represent the directions of the electric field in vacuum gap. "A", "B" and "C" represent the feet of different magnetic field lines (see text).



**Figure 2.** The potential barrier of electrons,  $\phi_p$ , in vacuum gap of typical NPs ( $P = 1 \text{ s}$ ,  $B = 10^{12} \text{ G}$ ). The potential energy of electrons at stellar surface, namely  $\phi_i(\theta)$ , is illustrated with fixed polar angles, for example, with  $0.6\theta_A$  and  $0.8\theta_A$ , where  $\theta_A$  is the polar angle of the feet of the last open field lines (Fig. 1).

**Table 1.** The polar angles of  $\theta_B$ ,  $\theta_C$  and  $\theta_0$  for both CR-induced and ICS-induced sparking of typical NPs and MSPs within both the choice of zero potentials.

	$\theta_A$ (rad)	$\theta_B$ ( $\theta_A$ )	$\theta_C$ ( $\theta_A$ )	$\theta_{0,B}$ ( $\theta_A$ )		$\theta_{0,C}$ ( $\theta_A$ )		
				CR	ICS	CR	ICS	
NPs	0.0145	0.69	0.76	0.49	... <sup>1</sup>	0.58	...	$\Omega \cdot \mathbf{B} > 0$
				0.84	2.76 <sup>2</sup>	0.90	2.83 <sup>2</sup>	$\Omega \cdot \mathbf{B} < 0$
MSPs	0.145	0.69	0.76	...	...	...	...	$\Omega \cdot \mathbf{B} > 0$
				1.49 <sup>2</sup>	...	1.52 <sup>2</sup>	...	$\Omega \cdot \mathbf{B} < 0$

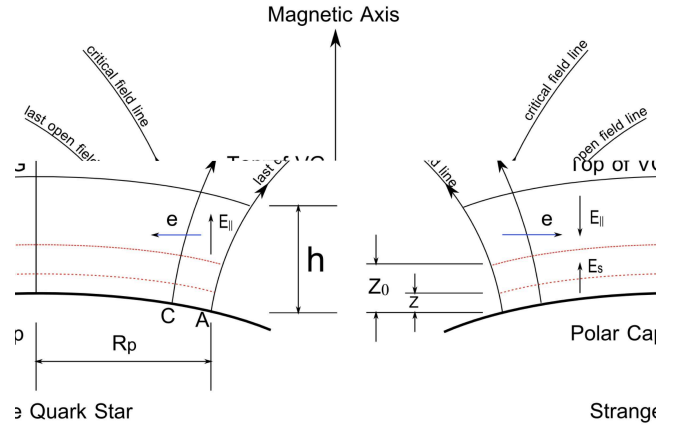
<sup>1</sup> $\theta_0$  does not exist, which means that the whole polar cap region is vacuum gap.<sup>2</sup> $\theta_0 > \theta_A$ , which means that the whole polar cap region is vacuum gap.**Figure 3.** Comparison between the total energy of electron on stellar surface with the height of the potential barrier of typical NPs with the choice of  $\phi_i(\theta_C) = 0$  and  $\phi_i(\theta_B) = 0$ , respectively. The solid horizontal line is the height of the potential barrier of electrons, namely  $\phi_P(Z = 0)$ .

### 2.3 The effects of thermionic emission and diffusion of electrons

It follows from the previous argument that electrons inside BSSs usually cannot stream into magnetospheres. Does any other process which may affect the existence of vacuum gap above polar cap? In vacuum gap, except pulling electrons from the interior of BSSs, two other processes which may also prevent vacuum gap from being formed are required to be investigated. One is the thermionic emission of electrons and another is the diffusion of electrons from the outer edge to the inner region of polar cap. For the first one, if the current density due to thermionic emission of electrons is much smaller than that of Goldreich-Julian charge density, the vacuum gap could be maintained as well. This current density is determined by the Richard-Dushman equation (Usov & Melrose 1995)

$$J_{th} = 1.2 \times 10^{14} T_6^2 \exp(-1.161 \times 10^4 T_6^{-1} \phi_{MeV}) \text{ A cm}^{-2}, \quad (8)$$

where  $m_e$  is the mass of electron,  $k_B$  is the Boltzmann constant,  $T_6 = T/(10^6 \text{ K})$  is the temperature and  $\phi_{MeV} = \phi/\text{MeV}$  is the work function of electrons. In the vacuum gap of BSSs, the work function of thermionic electrons is the order of the difference between the height of the potential barrier and the total energy of electron at the surface of BSSs. The order of the difference is about  $10^6 \text{ MeV}$ . At the

**Figure 4.** A representative illustration of the diffusion of electrons above the polar cap of bare strange quark star.

same time, the surface temperature of polar caps of BSSs is order of  $10^6 \text{ K}$ . Thus, the thermionic emission current density is  $\sim 0$ , which means that the thermionic emission of electrons cannot affect the existence of the vacuum gap.

The second process is the diffusion of electrons whose distribution above BSSs surface is (Xu et al. 2001)

$$n_e(Z) = \frac{1.187 \times 10^{32} \phi_{q,MeV}^3}{(0.06 \phi_{q,MeV} Z_{11} + 4)^3} \text{ cm}^{-3}. \quad (9)$$

Eq. 9 implies that the number density of electrons (so does the kinetic energy density,  $\epsilon_k$ ) decreases rapidly with increasing of the distance from quark matter surface at which  $\epsilon_k \gg \epsilon_B$ , where  $\epsilon_B$  is the magnetic field energy density. As a result, there is a balance surface where the kinetic energy density equals the magnetic energy density. Below this balance surface, electrons can cross magnetic field lines freely and above the balance surface, this motion is prevented. The physical picture of the diffusion of electrons is illustrated in Fig. 4. Making use of  $\epsilon_k = \epsilon_B$ , where  $\epsilon_k = n_e \epsilon_F$  ( $\epsilon_F$  is the Fermi energy of degenerate electrons) and  $\epsilon_B = B^2/8\pi$ , we can obtain the height of the balance surface. For NPs, it is  $Z_{11} \simeq 160$  and for MSPs, it is  $Z_{11} \simeq 1.7 \times 10^4$ , where  $Z_{11} = Z/(10^{-11} \text{ cm})$ . Keep in mind that there is a directed outward surface electric field above the quark matter surface. This surface electric field is much stronger than the gap electric field but decreases rapidly with also increasing of the distance. Which means that this surface electric field becomes smaller than the gap electric field above some certain

distance,  $Z_{0,11}$ . For NPs, it is  $Z_{0,11} \simeq 7000$ , and for MSPs, it is  $Z_{0,11} \simeq 6.3 \times 10^6$  (see Fig. 4). Both have  $Z_{11} \ll Z_{0,11}$  for NPs and MSPs. The diffusion of electrons beneath  $Z_{0,11}$  is still confined by the surface electric field meaning that only the diffusion of electrons above the surface with height of  $Z_{0,11}$  needs to be considered. The diffusion coefficient,  $D_c$ , is given by (Xu et al. 2001)

$$D_c \simeq \frac{\rho^2}{\tau_F} = \frac{\pi n_e c e^2}{B^2} = 2.17 \times 10^{-3} B_{12}^{-2} n_{e,29} \text{ cm}^2 \text{ s}^{-1}, \quad (10)$$

where  $\rho = \gamma \rho_L$  ( $\rho_L = m_e v c / (eB)$  is the Larmor radius) is the cyclotron radius of relativistic electrons, and  $\tau_F \simeq \gamma m_e^2 v^3 / (\pi e^4 n_e)$  is the mean free flight time of electrons. The gradient of electrons along with the diffusion direction is approximately

$$\frac{dn_e}{dx} \simeq \frac{n_e}{\rho} = 1.4 \times 10^{38} n_{e,29}^{2/3} \text{ cm}^{-4}. \quad (11)$$

Then, the diffusion rate is

$$I_{df} = 2.77 \times 10^{29} B_{12}^{-1} P^{-1/2} R_6^{3/2} \int_{Z_{0,11}}^{\infty} n_{e,29}^{5/3} dZ_{11} \text{ s}^{-1}, \quad (12)$$

where  $n_{e,29} = n_e / (10^{29} \text{ cm}^{-3})$ . For both the NPs and MSPs with different  $\phi_q$ , we give the results of the diffusion rate  $I_{df}$  and  $I_{GJ}$  in Table 2 in which the flow with the Goldreich-Julian flux is  $I_{GJ} = \pi r_p^2 c n_{GJ} \simeq 1.4 \times 10^{30} P^{-2} R_6^3 B_{12} \text{ s}^{-1}$ . we can know that both have  $I_{df} \ll I_{GJ}$  for NPs and MSPs from Table 2. This means that the diffusion of electrons is also negligible which guarantees the existence of vacuum gap.

### 3 CONCLUSIONS AND DISCUSSIONS

In RS75 model, the binding energy problem is one of the most serious problems in the normal neutron star model of pulsars. Arons and Scharlemann (1979) developed an alternative model, the space-charge limited flow (SCLF) model, in which the particles, both iron ions and electrons can be pulled out freely, and form a steady flow (Aron & Scharlemann 1979). In this SCLF model, the drifting sub-pulse phenomenon which has been commonly observed in pulsars can rarely be reproduced. The prerequisite for understanding this phenomenon could be the existence of a vacuum gap.

In a very special case, through our calculations, we find that there is a new physical scenario for CR-induced sparking of normal pulsars (NPs) that free flow and vacuum gap may coexist above the polar cap. But in other cases, such as ICS-induced sparking of NPs and millisecond pulsars (MSPs), only vacuum gap exists. In general, if a pulsar is not highly negatively charged (Xu et al. 2006), vacuum gap survives at polar cap as well. One limitation is that our calculation is based on one-dimensional approximation and it might fail in some cases of MSPs. As far as we find, it is very difficult to deal with the high-dimensional cases. The one-dimensional approximation provides a good understanding of the geometry of polar cap of BSSs. In conclusion, the binding energy problem could be solved completely in the BSS model of pulsar as long as BSSs are neutral (or not highly negative charged), and the structure of polar cap of BSSs are very different with respect to that of NSs. Detailed information about the geometry of BSS's polar cap is given

in Table 3. A more interesting region from pole to equator may locate between that polar angle where the total energy of electron equals the potential barrier and the polar angle of the foot of zero potential magnetic field line (i.e.,  $[\theta_{0,C}, \theta_C]$  or  $[\theta_{0,B}, \theta_B]$ , see Fig. 3) for CR-induced sparking NPs. After the birth of a NP, a vacuum gap exists at this region. When sparking starts, the potential in vacuum gap drops rapidly due to screen by electron-positron pairs and may become lower than that at the surface, namely  $V_i(\theta)$ . As a result, the sparking converts vacuum gap to free flow at this region until the sparking ends, i.e., at  $[\theta_{0,C}, \theta_C]$  or  $[\theta_{0,B}, \theta_B]$ , vacuum gap and free flow work alternately. This argument may have profound implications for us to distinguish neutron stars and quark stars by pulsar's magnetospheric activities (e.g., the diversity pulse profiles).

Another issue to be discussed is about the drifting rate of subpulses when we use the height of pure vacuum gap in this work. The natural explanation of the drifting subpulse phenomena in vacuum gap is due to  $\mathbf{E} \times \mathbf{B}$ . Unfortunately, these theoretical calculations gave higher drifting rate with respect to observations (e.g., Ruderman & Sutherland 1975; Deshpande & Rankin 1999, 2001; Gil et al. 2003, 2006b). Since it has been observed (Drake & Craft 1968), the drifting subpulse phenomenon remains unclear which has been widely regarded as one of the most critical and potentially insightful aspects of pulsar emission (Deshpande & Rankin 2001). The PSG mechanism (e.g., Gil et al. 2003, 2006a,b) could be a way to understand lower drifting rates observed, but some complexities still exist which make the underlying physics of drifting subpulses keep complicated and far from knowing clearly. (1) in principle the drifting velocity of subpulses is the ratio of the drifting distance to the duration, while the expected velocity predicted by  $\mathbf{E} \times \mathbf{B}$  is only for electrons in separated emission units, namely the plasma filaments. These two velocities would not be the same if the plasma filaments may stop after sparking. When sparking starts, the electric field in the vacuum gap vanishes due to screen by plasmas; while sparking ends, the electric field appears again. Thus, the calculated drifting velocity with  $\mathbf{E} \times \mathbf{B}$  could be higher than that of observations. (2) the so-called aliasing effect: as one observes subpulses only once every rotation period, we can hardly determine their actual speed. The main obstacles in the aliasing problem are the under sampling of subpulse motion and our inability to distinguish between subpulses especially when the differences between subpulses formed by various subbeams are smaller than the fluctuations in subpulses from one single subbeam (van Leeuwen et al. 2003). Anyway, detailed studies are very necessary in the future works.

We assume that the potential energy related to Eq. 2,  $eV_i$ , to be the constant,  $\phi_0$ , in Eq. 1. This assumption could be reasonable. For an uniformly magnetized, rotating conductor sphere, the unipolar generator will induce an electric field which is a function of polar angle, as described in Eq. 2. In the case of  $\mathbf{\Omega} \cdot \mathbf{B} > 0$  (Fig. 1), the potential energy of electron is highest at the polar region which means that those electrons there could be easier to escape. Alternatively, this conclusion could be quantitatively understood as following: because of Lorentz force inside a star, more electrons locate at the polar region so that the Fermi energy of electron is higher there and easier to escape into magnetosphere.

**Table 2.** The typical value of the diffusion rate for NPs and MSPs with different choice of  $\phi_q$ .

$\phi_q$ (MeV)	NPs		MSPs	
	$I_{df}$ ( $10^{24} \text{ s}^{-1}$ )	$I_{GJ}$ ( $10^{24} \text{ s}^{-1}$ )	$I_{df}$ ( $10^{17} \text{ s}^{-1}$ )	$I_{GJ}$ ( $10^{17} \text{ s}^{-1}$ )
1	$\sim 4.75$		$\sim 7.52$	
10	$\sim 4.91$	$\sim 1.4 \times 10^3$	$\sim 7.52$	$\sim 1.4 \times 10^{13}$
20	$\sim 4.93$		$\sim 7.53$	

**Table 3.** The accelerators above polar caps of BSSs.

	$[0, \theta_0]^\dagger$		$[\theta_0, \theta_A]$		
	CR	ICS	CR	ICS	
NPs	SCLF	VG	VG	VG	$\mathbf{\Omega} \cdot \mathbf{B} > 0$
	VG	VG $^\ddagger$	SCLF	VG $^\ddagger$	$\mathbf{\Omega} \cdot \mathbf{B} < 0$
	VG	VG	VG	VG	$\mathbf{\Omega} \cdot \mathbf{B} > 0$
MSPs	VG $^\ddagger$	VG	VG $^\ddagger$	VG	$\mathbf{\Omega} \cdot \mathbf{B} < 0$

$^\dagger \theta_0$  represents  $\theta_{0,B}$  while choosing  $\phi_B = 0$  and  $\theta_{0,C}$  while choosing  $\phi_C = 0$ .

$^\ddagger$  for such cases,  $\theta_0 > \theta_A$ , which represents the structure of the whole polar cap region.

## ACKNOWLEDGMENTS

We thank Dr. Kejia Lee and other members in the pulsar group of Peking University for their helpful and enlightened discussions. We also thank Prof. Janusz Gil for his helpful comments and suggestions. Junwei Yu is grateful to Dr. Caiyan Li for her helpful assistance. The work is supported by NSFC (10973002, 10935001), the National Basic Research Program of China (grant 2009CB824800) and the John Templeton Foundation.

## REFERENCES

- Alcock, C. Farhi, E. & Olinto, A. 1986, ApJ, 310, 261  
Arons, J. & Scharlemann, E. T. 1979, ApJ, 231, 854  
Deshpande, A. A. & Rankin, J. M. 1999, ApJ, 524, 1008  
Deshpande, A. A. & Rankin, J. M. 2001, MNRAS, 322, 438  
Drake, F. D. & Craft, H. D. 1968, Nature 220, 231  
Fowlers, E. G. Lee, J. F. Ruderman, M. A. Sutherland, P. G. Hillebrandt, W. & Muller, E. 1977, ApJ, 215, 291  
Gil, J. Melikidze, G. I. & Geppert, U 2003, A&A, 407, 315  
Gil, J. Melikidze, G. & Zhang, B. 2006, ApJ, 650, 1048  
Gil, J. Melikidze, G. & Zhang, B. 2006, ChJAS, 6, 105  
Gil, J. Haberl, F. Geppert, U. Zhang, B. & Melikidze, G. Jr. 2008, ApJ, 686, 497  
Goldreich, P. & Julian, W. H. 1969, ApJ, 157, 869  
Lai, D. 2001, Rev. Mod. Phys., 73, 629  
van Leeuwen, A. G. J. Stappers, B. W. Ramachandran, R. & Rankin, J. M. 2003, A&A, 399, 223  
Medin, Z. & Lai, D. 2007 MNRAS, 382, 1833  
Melikidze, G. & Gil, J. 2009, The Eighth Pacific Rim Conference on Stellar Astrophysics ed B Soonthornthum, S. Komonjinda, Cheng, K. S. & Leung K. C. (San Francisco: Astronomical Society of the Pacific) 73, 131  
Qiao, G. J. Lee, K. J. Zhang, B. Xu, R. X. & Wang, H. G. 2004, ApJ, 616, 127  
Qiao, G. J. & Lin, W. 1998, A&A, 333, 172  
Ruderman, M. A. & Sutherland, P. G. 1975, ApJ, 196, 51  
Shukre, C. S. 1992, Magnetospheric Structure and Emission Mechanisms of Radio Pulsars, (IAU Colloq. 128) ed T H Hankins, J. M. Rankin, J. M. & Gil, J. A. (Pedagogical Univ. Press) p.412  
Usov, V. V. & Melrose, D. B. 1995, Aust. J. Phys., 48, 571  
Vivekanand, M. & Joshi, B. C. 1999, ApJ, 515, 398  
Xu, R. X. 2009, J. Phys. G: Nucl. Part. Phys., 36, 064010  
Xu, R. X. 2010, Int. Jour. Mod. Phys., D19, 1437  
Xu, R. X. Cui, X. H. & Qiao, G. J. 2006, Chin. J. Astron. Astrophys., 2, 217  
Xu, R. X. & Qiao, G. J. 1998, Chin. Phys. Lett. 15, 934  
Xu, R. X. Qiao, G. J. & Zhang, B. 1999, ApJ, 522, L109  
Xu, R. X. Zhang, B. & Qiao, G. J. 2001, Astropart. Phys., 15, 101  
Zhang, B. Harding, A. K. & Muslimov, A. G. 2000, ApJ, 531, L135